Published in final edited form as:
*Cell Rep*. 2012 October 25; 2(4): 866–877. doi:10.1016/j.celrep.2012.08.036.

# A Gradient of ATP Affinities Generates an Asymmetric Power Stroke Driving the Chaperonin TRIC/CCT Folding Cycle

**Stefanie Reissmann**[1,2,3], **Lukasz A. Joachimiak**[1,*,2], **Bryan Chen**[1], **Anne S. Meyer**[1,4], **Anthony Nguyen**[1], and **Judith Frydman**[1,*]

[1]Department of Biology and BioX Program, Stanford University, Stanford, CA 94305-5020, USA

## SUMMARY

The eukaryotic chaperonin TRiC/CCT uses ATP cycling to fold many essential proteins that other chaperones cannot fold. This 1 MDa hetero-oligomer consists of two identical stacked rings assembled from eight paralogous subunits, each containing a conserved ATP-binding domain. Here, we report a dramatic asymmetry in the ATP utilization cycle of this ring-shaped chaperonin, despite its apparently symmetric architecture. Only four of the eight different subunits bind ATP at physiological concentrations. ATP binding and hydrolysis by the low-affinity subunits is fully dispensable for TRiC function in vivo. The conserved nucleotide-binding hierarchy among TRiC subunits is evolutionarily modulated through differential nucleoside contacts. Strikingly, high-and low-affinity subunits are spatially segregated within two contiguous hemispheres in the ring, generating an asymmetric power stroke that drives the folding cycle. This unusual mode of ATP utilization likely serves to orchestrate a directional mechanism underlying TRiC/CCT's unique ability to fold complex eukaryotic proteins.

## INTRODUCTION

The chaperonin TRiC/CCT is stringently required to maintain cellular protein homeostasis in eukaryotic cells (Hartl et al., 2011; Tyedmers et al., 2010). This large, ring-shaped chaperonin plays a central role in folding of newly translated polypeptides (Thulasiraman et al., 1999; Yam et al., 2008), as well as in prevention of protein aggregation (Kitamura et al., 2006; Tam et al., 2006) and regulation of the stress response (Neef et al., 2010). TRiC assists in the cotranslational folding of many different poly-peptides with complex topologies, and is required for the folding of cytoskeletal proteins and cell-cycle regulators (Camasses et al., 2003; Tian et al., 1995; Yam et al., 2008). Remarkably, no other chaperone, not even the structurally related bacterial and archaeal chaperonin systems, are capable of replacing TRiC/CCT in the folding of some of its substrates, such as actin and tubulin (Hartl et al., 2011; Tian et al., 1995).



*Correspondence: lajoachi@stanford.edu (L.A.J.), jfrydman@stanford.edu (J.F.).
[2]These authors contributed equally to this work
[3]Present address: Max Planck Institute for Terrestrial Microbiology, 35043 Marburg, Germany
[4]Present address: Kavli Institute of Nanoscience, Delft University of Technology, 2628 CJ Delft, The Netherlands

SUPPLEMENTAL INFORMATION

Supplemental Information includes Extended Experimental Procedures, seven figures, and four tables and can be found with this article online at http://dx.doi.org/10.1016/j.celrep.2012.08.036.

TRiC is a 16-mer, 1 MDa, group II chaperonin composed of two identical stacked rings of eight paralogous subunits each. Each subunit contains a segment that functions as a built-in lid over the central ring chamber, which accommodates substrate proteins (Bigotti and Clarke, 2008; Horwich et al., 2007; Spiess et al., 2004). TRiC-mediated folding is a nucleotide-dependent process whereby ATP binding and hydrolysis regulate an elaborate conformational cycle that leads to opening and closing of the built-in lid and encapsulation of substrate within the central chamber, where it folds (Booth et al., 2008; Cong et al., 2011). The eight paralogous subunits of TRiC share on average only 27%–39% sequence identity but have the same three-domain arrangement. The equatorial domains provide the interring contacts and harbor the ATP-binding pocket. The hinge-like intermediate domains cover the ATP-binding pocket from the top and communicate ATP-induced conformational changes to the distal apical domains where the substrate-binding sites are located. Protrusions extending from the very tip of the apical domains in every subunit assemble into the iris-like lid structure that closes over the central cavity upon ATP hydrolysis, resulting in the folding active state. Recent studies elucidating the elaborate hetero-oligomeric architecture of TRiC showed that it contains two identical rings related by a 2-fold symmetry axis through two homotypic subunit contacts (Leitner et al., 2012). These studies further uncovered an additional axis of symmetry in the charge distribution within the central folding chamber, which may relate to TRiC's unique ability to fold some eukaryotic proteins.

The regulation of the conformational cycle of TRiC is poorly understood. Assembly of the iris-like lid structure from building blocks provided by the paralogous subunits involves ATP-induced conformational changes that must be highly coordinated. Indeed, the subunits within one ring form an allosteric unit coupled through the lid to yield intraring positive cooperativity (Kafri et al., 2001; Reissmann et al., 2007). One important unresolved issue is how each of the paralogous subunits within a ring contribute to the ATP-driven conformational cycle. On one hand, the equatorial domain of TRiC subunits is highly conserved and key features of the ATP-binding pocket, like the phosphate-binding loop (P loop) and residues involved in catalysis, are absolutely conserved in all TRiC subunits and their archaeal paralogs, suggesting a symmetric contribution to the ATPase cycle (Archibald et al., 2001; Kim et al., 1994). On the other hand, early experiments indicated that equivalent mutations in the P loop of two yeast TRiC/CCT subunits exhibited distinct phenotypes (Lin et al., 1997). Additionally, replacement of the catalytic aspartic acid by a bulkier but still negatively charged glutamic acid also produced different growth phenotypes in different subunits (Amit et al., 2010), raising the possibility of more complex regulation.

Here we combine biochemical, computational, and genetic approaches to investigate how nucleotide binding to the different TRiC subunits contributes to its functional cycle. Our data indicate that each subunit in the TRiC complex plays a unique and evolutionarily conserved role in its conformational cycle. We find that only a subset of TRiC subunits binds nucleotide under conditions in which the complex exhibits maximal folding activity. Whereas ATP binding to these high-affinity subunits is required for viability, ATP binding to the four low-affinity subunits is dispensable for TRiC activity. Notably, high-and low-affinity subunits segregate spatially within the ring into two contiguous hemispheres to create an axis of symmetry. Our findings offer a new perspective on how evolutionary forces have imparted a highly asymmetric functional cycle to this seemingly symmetric complex. The hetero-oligomeric nature of the ring has allowed the modulation of ATP occupancy to create a unique mode of asymmetric ATP utilization that has not yet been observed for other hetero-oligomeric ring-shaped complexes. We propose that this provides the possibility for regulation and directionality of the conformational cycle.

# RESULTS

## Substoichiometric ATP Usage by the Eukaryotic Chaperonin TRiC

To understand how TRiC uses ATP, we initially used a size exclusion chromatography (SEC) approach to determine the nucleotide-binding stoichiometry of the TRiC complex at 1 mM α-[$^{32}$P]-ATP (herein termed ATP*), a saturating nucleotide concentration that promotes nucleotide binding to both rings (Figure 1A; Booth et al., 2008; Reissmann et al., 2007). Surprisingly, the TRiC 16-mer binds on average only seven nucleotides (Figure 1B, ATP*). To prevent the possible dissociation of ATP or ADP, we next used α-[$^{32}$P]-8-$N_3$-ATP (herein termed azATP*), which binds TRiC with similar affinity as ATP (Figure S1A) but forms covalent adducts upon photolysis. We optionally also included $AlF_x$ during incubation with either ATP* or azATP* to trap TRiC in the ATP-induced symmetrically double-closed state (Booth et al., 2008; Meyer et al., 2003). In the presence of ATP$AlF_x$, TRiC lid segments were insensitive to protease treatment, indicative of a symmetrically closed state (Figure 1C). This symmetrically closed TRiC bound only 7–9 nucleotides per 16-mer, even after covalent ATP crosslinking (Figure 1B). Importantly, control experiments using the well-studied 14-mer bacterial chaperonin GroEL in complex with its cofactor GroES (Horwich et al., 2006) yielded the expected nucleotide stoichiometry. For instance, singly capped GroEL-GroES complexes obtained by incubation with ATP yielded ~7 nucleotides per GroEL 14-mer (Table S1), whereas incubation with ATP$AlF_x$, which generates a doubly capped GroEL-$(GroES)_2$ complex, yielded 14 nucleotides per GroEL 14-mer (Table S1; Bochkareva et al., 1992; Taguchi et al., 2004). Thus, unlike GroEL, TRiC achieves double-ring closure at substoichiometric nucleotide occupancy, suggesting that not all subunits contribute equally to the ATPase cycle.

## Only a Subset of the Eight Different Subunits Binds to ATP under Saturation Conditions

We next considered the molecular basis for the substoichiometric nucleotide occupancy in doubly closed TRiC. In principle, ATP could bind stochastically to any subunit until a threshold sufficient for lid closure is achieved, at which point binding to more subunits would be disfavored (Jiang et al., 2011). Alternatively, hierarchical or selective binding could preferentially direct ATP to some subunits, disfavoring binding to others. These models make distinct predictions for subunit occupancy. In the stochastic model, ATP randomly binds to all subunits in a concentration-dependent manner, whereas in the hierarchical model, ATP preferentially binds to a subset of subunits with higher affinity. We crosslinked azATP* to purified bovine TRiC at saturating concentrations and identified the individual subunits in contact with nucleotide through a combination of reverse-phase high-performance liquid chromatography (RP-HPLC), SDS-PAGE, and mass spectrometry (Spiess et al., 2006; Figures 1D–1F and S1B).

Strikingly, at 1 mM azATP*, only four subunits (CCT5, CCT4, CCT1, and CCT2) significantly crosslinked to nucleotide (Figure 1E). In contrast, little azATP* was detected for CCT3, CCT6, CCT7, and CCT8 (Figures 1E and S1B). Similar crosslinking results were obtained following incubation with azATP*$AlF_x$, which produces stable, symmetrically closed TRiC complexes (Figure 1F). Furthermore, the ATP occupancy and ATPase rates of TRiC were unaffected by stoichiometric binding of the stringent substrate actin (Figure S2). It thus appears that nucleotide occupancy in only four subunits suffices to drive the ATPase cycle of TRiC and to generate symmetrically closed complexes. These experiments account for the observed stoichiometry of eight nucleotides per 16-mer TRiC complex at saturating nucleotide concentrations. Of note, they may also explain the unequal nucleotide density observed in recent low-resolution TRiC structures (Dekker et al., 2011; Muñoz et al., 2011).

## Hierarchy of ATP Affinities for the Eight Paralogous Subunits of TRiC

Our data support a model in which double-ring closure is achieved by selective association of ATP with four specific subunits in each ring. To test whether all of the high-affinity subunits display similar or different affinities for ATP, we cross-linked ATP to TRiC using α-[$^{32}$P]-8N$_3$-ATP at low (10 μM), intermediate (0.2 mM, 0.5 mM), or high (1 mM, 2 mM) nucleotide concentrations (Figure 2). In a previous study that investigated allostery in TRiC, the ATPase activity of the bovine TRiC complex was measured as a function of ATP concentration (Figure 2A; Reissmann et al., 2007). It was shown that at very low ATP concentration (10 μM), only a small fraction of TRiC molecules hydrolyze ATP, whereas at 0.2 mM ATP, all TRiC molecules hydrolyze ATP within one ring. Higher, saturating ATP concentrations (1 mM and 2 mM ATP) overcome the negative interring cooperativity so that both rings bind to ATP. Notably, nucleotide occupancy in both rings results in a reduction of the overall ATPase rate (Reissmann et al., 2007). The crosslinking experiments carried out at these ATP concentrations indicated a wide range of nucleotide affinities for the different TRiC subunits. At very low ATP concentrations (10 μM), only CCT5 and, to a lesser extent, CCT4 crosslinked to ATP (Figure 2B). Increasing the nucleotide to 0.2 mM enhanced crosslinking to CCT4 (Figure 2C). At 0.5 mM ATP, two additional subunits (CCT1 and, to a lesser extent, CCT2) crosslinked to ATP (Figure 2D). Only at very high ATP concentrations, well above those required for maximal ATPase rates (i.e., 2 mM; Kafri et al., 2001; Reissmann et al., 2007), did we observe crosslinks to some low-affinity subunits (Figure 2E), indicating that the low-affinity subunits can, in principle, bind and crosslink to nucleotide. Importantly, maximal ATP hydrolysis and substrate folding rates are observed at 0.3 mM ATP (Figure 2A; Reissmann et al., 2007), demonstrating that full nucleotide occupancy is not required for optimal TRiC function. We conclude that a gradient of affinities governs ATP binding to TRiC subunits: CCT5 and CCT4 have the highest affinities and thus are occupied at the lowest ATP concentrations, followed by CCT1 and CCT2. However, CCT3, CCT6, CCT7, and CCT8 have very low ATP occupancy even at high ATP concentrations, and thus are classified as low-affinity subunits (Figure 2F).

## Unequal Active-Site Conservation across TRiC Paralogs Suggests that Nucleoside Contacts Modulate Affinity

The stark segregation of TRiC subunits into high- and low-ATP-affinity regimes is surprising, given the high conservation of ATP-binding domains (Kim et al., 1994). To provide a rationale for the observed affinity differences, we identified amino acid residues that contributed to the first shell of ATP contacts (within 5 Å) in different TRiC paralogs (Figures 3A, 3B, S3A, and S3B). Next, we evaluated the conservation of this minimal ATP-binding pocket among the different paralog subunits of bovine and yeast TRiC. Normalized per-residue conservation scores were computed for all residues within the first shell of interactions, as well as for residues contacting only the triphosphate or the nucleoside moieties (ATP, PPP, and nucleoside; Figures 3B and 3C). Residues contacting the triphosphate were highly conserved; however, residues contacting the nucleoside were quite variable among the different subunits in both yeast and bovine TRiC (Figures 3C). Mapping these conservation scores onto structural models of the minimal ATP-binding pocket clearly illustrates the high variability within the nucleoside contacting residues (Figures 3D and 3E). We hypothesize that these differential nucleoside contacts could account for the observed ATP occupancy differences among TRiC subunits. The observed differential conservation of triphosphate and nucleoside contacts between TRiC subunits is not restricted to bovine and yeast TRiC, and appears even more dramatically preserved when one compares all TRiC paralogs from 100 different eukaryotic species (Figure 3C). Of note, the ATP-binding sites of archaeal chaperonins also exhibit significant variability in amino acids contacting the nucleoside, and high conservation within triphosphate-contacting residues (Figures S3C and

S3D), suggesting that this may be a widespread strategy that arose early in group II chaperonin evolution.

## High-Affinity TRiC Orthologs Have Highly Conserved Nucleoside Contacts

If nucleoside contacts indeed modulate ATP affinity, the high variability of these contacts in different subunits may serve an evolutionarily conserved function. We thus asked whether high-affinity subunits are under stronger evolutionary pressure to maintain suitable nucleoside contacts than low-affinity subunits. An analysis of orthologous sequences across 100 different species revealed that nucleoside-binding contacts are in fact more conserved in high-affinity subunits than in low-affinity subunits (Figures 4A, 4B, and S4A). This strongly indicates that preferential nucleotide binding to high-affinity subunits is functionally important. The highest conservation was always observed for the nucleoside-binding contacts of CCT4 (Figures 4B and 4C), suggesting that this subunit plays a key role in the ATPase cycle, followed by CCT5. The highest diversity among nucleoside contacts was consistently observed for CCT6 (Figures 4B and 4D), which was not observed to crosslink to ATP for the bovine complex even at the highest nucleotide concentration (Figure 2E).

Ideally, the affinity of single subunits for ATP would be determined experimentally; however, individual TRiC subunits cannot be stably expressed in isolation (data not shown). Therefore, we exploited recent advances in ligand docking algorithms (Davis and Baker, 2009) to examine the nucleotide-binding energetics for individual subunits. First, we evaluated the algorithms' ability to correctly predict the orientation of ATP in experimentally determined structures of archaeal group II chaperonins. The docking approach successfully recapitulated the ATP binding orientation observed in both the α and β thermosome (Ths) structures (Ditzel et al., 1998) (all-atom root-mean-square deviation [rmsd] = 0.31 Å and 0.18 Å for Thsα and Thsβ, respectively; not shown). Of note, the docking procedure suggested that Thsα binds ATP more tightly than Thsβ (as shown by the lower $\Delta G_{calc}$; Figure 4E), a prediction that is consistent with previous experimental findings (Gutsche et al., 2000). We next applied this docking approach to TRiC subunits using the experimentally determined structures of each of the yeast TRiC subunits in the nucleotide-bound conformation (Leitner et al., 2012) and homology models for each of the bovine TRiC subunits (see Extended Experimental Procedures for details). Application of this docking protocol to TRiC subunits predicted that bovine as well as yeast high-affinity subunit CCT4 can bind ATP more tightly than low-affinity subunits such as CCT3 (Figures 4E, S4B, and S4C), consistent with our experimental observations (Figures 1 and 2). Given the lack of detailed structural information for subunits in the ATP-free open TRiC complex, which is the conformation that binds nucleotide, these docking experiments were performed with isolated subunits in the better-defined, closed conformation, and therefore are only a coarse approximation for the actual binding energies of ATP. Nonetheless, these analyses support the idea that nucleoside contacts are evolutionarily tuned to regulate subunit affinity and binding energy for ATP.

## A Hierarchy of ATP Binding to TRiC Paralogs Governs Chaperonin Function In Vivo

To examine the relevance of the observed ATP-binding hierarchy among TRiC subunits for its function in vivo, we systematically disrupted ATP binding (Figure 5A) in each of the eight yeast subunit paralogs. To that end, we replaced the entire P loop (GDGTT) with a stretch of five alanines (herein termed the BND mutation; Figure 5A; Amit et al., 2010; Fenton et al., 1994; Lin et al., 1997; Weiss and Goloubinoff, 1995). Introducing the BND mutation into any of the high-affinity subunits identified by our biochemical analyses (i.e., CCT4, CCT5, CCT1 and CCT2) was lethal (Figure 5B). In contrast, introducing BND into the low-affinity subunits (i.e., CCT3, CCT7, CCT6, and CCT8) had no effect on growth (Figure 5B; Table S2), even under conditions that stress TRiC function, such as benomyl

treatment (Figure S5A). Furthermore, stringent pulse-chase analyses in yeast cells carrying the relevant mutations indicated that neither the folding rate of newly translated actin (Figures 5C and 5D for CCT6) nor the flux of newly translated polypeptides through TRiC (Figure 5E for CCT6) were affected by introducing the BND mutation into low-affinity subunits. These functional analyses were consistent with further biochemical tests to assess whether the chaperonin complexes carrying BND mutations in single subunits were able to close their built-in lids upon incubation with ATP (Figure 5F for CCT6). For these tests, cell extracts from the respective mutant yeast strain were incubated in the absence or presence of hydrolyzable nucleotide, resolved by nondenaturing gel electrophoresis, and the migration behavior of TRiC complexes was analyzed by immunoblot (Leitner et al., 2012; Meyer et al., 2003). In the absence of nucleotide, the TRiC complex remains open and migrates with lower mobility during nondenaturing electrophoresis (Figure 5F; O, open conformation). However, addition of ATPAlFx stabilizes the doubly closed TRiC complex, resulting in a characteristic faster mobility of the complex (Figure 5F; C, closed conformation). Indeed, non-denaturing gel electrophoresis confirmed that impairing ATP binding in low-affinity subunits does not prevent TRiC closure (Figure 5F for CCT6). We conclude that TRiC function in vivo only requires ATP binding to the high-affinity subunits.

To further examine the functional hierarchy of ATP binding among high-affinity subunits, we introduced a milder ATP-binding mutation by only replacing the P-loop aspartic acid with alanine ($D_{Ploop}$, herein termed Bnd*; Figure 5A; Fenton et al., 1994; Weiss and Goloubinoff, 1995). As expected from the lack of effect of the more-dramatic BND mutations, the milder Bnd* mutation did not affect viability when introduced into the low-affinity subunits (Figure 5B; Table S2). Notably, introducing the Bnd* mutation had little (CCT5) or no (CCT1 and CCT2) effect in three of the four high-affinity subunits, even under TRiC stress (Figure S5B). Native gel electrophoresis confirmed that impairing ATP binding in CCT5, CCT1, and CCT2 using the Bnd* mutation did not prevent TRiC closure (Figures 5G and S5C). In contrast, introduction of the Bnd* mutation into the high-affinity subunit CCT4 abolished TRiC function and was lethal (Figure 5B). The sensitivity of CCT4 to this milder mutation suggests a central role for this subunit in the progression of the TRiC conformational cycle.

## Hierarchical Role of ATP Hydrolysis by TRiC Paralogs In Vivo

We next examined whether the requirement for ATP hydrolysis within the different TRiC paralogs also follows a hierarchical pattern. To that end, we substituted the universally conserved catalytic aspartic acid with an alanine ($D_{cat}$ to A; Figure 6A). Introducing this mutation (herein termed HYD) into either GroEL or homo-oligomeric archaeal group II chaperonins fully blocks ATP hydrolysis and lid closure without affecting ATP binding (Douglas et al., 2011; Reissmann et al., 2007; Rye et al., 1999). Notably, introducing the HYD mutation into any of the low-affinity subunits did not impair viability, even under conditions of TRiC stress, such as growth on benomyl (Figures 6B and 6C; Table S2). Thus, disrupting ATP binding or hydrolysis in these low-affinity subunits does not affect TRiC function in vivo. In contrast, introducing the HYD mutation into the high-affinity subunits caused a hierarchy of phenotypes (Figures 6B and 6C). Cells carrying CCT4 HYD were not viable (Figure 6B), CCT5 HYD cells were severely affected (Figures 6B–6D), and CCT1 HYD cells had a mild growth defect, whereas CCT2 HYD cells grew normally (Figures 6B and 6C, Table S2). The growth defects in CCT1 HYD and CCT5 HYD cells were linked to TRiC function, given their hypersensitivity to TRiC stresses (Figure 6C) and their abnormally high DNA content, which are typical of TRiC mutants (Figure S6; Camasses et al., 2003). Because ATP hydrolysis is absolutely required for lid closure (Douglas et al., 2011; Meyer et al., 2003; Reissmann et al., 2007), we next examined whether the HYD mutations in different subunits affected lid closure of the TRiC complex upon incubation

with ATP. All viable HYD mutants, except CCT5 HYD, could fully achieve the closed state upon incubation with ATP·$AlF_X$ (Figure 6E). A notable exception was CCT5 HYD, since in this case lid closure was substantially impaired (Figure 6E). It thus appears that inability to hydrolyze ATP in CCT5 stalls the conformational cycle, consistent with its very severe growth defect (Figures 6B–6D). Our results indicate that the necessity to hydrolyze bound ATP in the different TRiC subunits is also hierarchically distributed. Nucleotide hydrolysis in CCT4 and, to a lesser extent, CCT5 is absolutely essential for TRiC function. Of note, ATP hydrolysis by the other subunits is not stringently required to close the lid.

## DISCUSSION

Taken together, the experiments presented here reveal an unusual diversification in the role of the different subunits of the ring in the eukaryotic chaperonin. Biochemical, evolutionary, and in vivo analyses delineate the hierarchical nature of the TRiC ATPase cycle and its relevance to chaperonin function in the cell. CCT4 and CCT5 are the two subunits with the highest nucleotide affinity, as determined via azATP crosslinking studies (Figures 1 and 2). Notably, nucleotide binding and hydrolysis mutations in these subunits also have the strongest effect on TRiC function in vivo (Figures 5 and 6). ATP binding or hydrolysis in the low-affinity subunits was entirely dispensable for function, consistent with biochemical (Figures 1 and 2) and bioinformatic analyses (Figures 3 and 4). The hierarchical contribution of TRiC subunits to the conformational cycle appears to be an evolutionarily conserved feature modulated through diversification of the nucleoside contacts, and is an unprecedented instance of asymmetric ATP usage by a ring-shaped hetero-oligomer.

### High- and Low-Affinity Subunits Segregate Asymmetrically into Two Hemispheres within the Ring

Interpreting our findings in light of the TRiC subunit arrangement and structure recently elucidated by Leitner et al. (2012) reveals a striking asymmetry in ATP utilization within the complex (Figure 7). Mapping the subunit-specific biochemical, computational, and functional properties defined in this study onto the TRiC structure uncovers an axis of symmetry that segregates high-affinity from low-affinity subunits into two contiguous hemispheres with similar properties (Figures 7A–7C). Side views indicate that the high- and low-affinity hemispheres are almost in register between the rings, staggered by only one subunit (Figures 7C and S7A). In this register, the two highest-affinity subunits, CCT4 and CCT5, form interring contacts, as does the lowest-affinity subunit, CCT6. The staggered register results in a single high-/low-affinity interring pairing, i.e., CCT1/CCT7 (Figure S7A). The spatial asymmetry creates high- and low-ATP-utilization regions within the complex, which likely underlie its unique regulation and allosteric properties.

Strikingly, we find that the asymmetric ATP utilization is absolutely conserved from yeast to mammals. An interesting question for future studies is, how did such a dramatic asymmetry in the ATP utilization cycle evolve from symmetric ancestral chaperonins? Phylogenetic analyses of eukaryotic TRiC subunit sequences demonstrate that the two subunits most essential to the ATPase cycle, CCT4 and CCT5, belong to the same evolutionary clade. Because these subunits also engage in interring contacts, their coevolution may have played a role in regulating interring cooperativity. In support of this idea, the interring pair CCT1 and CCT7 also belong to an evolutionary clade (Figure S7B). Although we observe dramatic differences between the high- and low-affinity subunits in terms of ATP occupancy and functional relevance, we are unable to directly measure the intrinsic affinity for nucleotide of an individual subunit in isolation. In principle, a slight difference in affinity, mediated by more favorable nucleoside contacts, could translate into the observed dramatic difference in occupancy. For instance, if ATP binding to a few higher-affinity subunits were sufficient to trigger the closed conformation, the requirement

for ATP binding in the lower-affinity subunits would become less stringent or even sterically disfavored. This could provide a rationale for the reduced selective pressure to maintain favorable nucleoside contacts in the lower-affinity subunits. Once it became established, the subunit-specific ATP utilization may have evolved further to establish directionality in the conformational change and to provide additional regulation through further diversification of the subunits.

### A Gradient of Nucleotide Affinities Generates an Asymmetric Power Stroke

Our results provide insights into how the diversification of subunits in the ring-shaped eukaryotic chaperonin changed the mechanics that link ATP hydrolysis to the conformational cycle (Figure 7D). Symmetrical, homo-oligomeric ring-shaped complexes do not have a clear register that would define an initiation point for their conformational cycle. In contrast, the unique properties of TRiC subunits for nucleotide binding and hydrolysis create a highly asymmetric power stroke. The hierarchical mode of ATP utilization is evolutionarily hard-wired into the oligomer topology to initiate the power stroke in the high-affinity hemisphere and to propagate the conformational change throughout the entire ring. In principle, the asymmetric binding of nucleotide is consistent with both a concerted (Monod-Wyman-Changeux [MWC]) and a sequential (Koshland-Nemethy-Filmer [KNF]) mode of conformational change. Of note, based on an analysis of negative-stain electron microscopy (EM) images of TRiC, Rivenzon-Segal et al. (2005) proposed that lid closure occurs sequentially following a KNF allosteric model. Remarkably, a reinterpretation of their data using the subunit ordering described by Leitner et al. (2012) reveals that the lobe of subunits that initiate the ATP-induced conformational changes correspond to the high-affinity subunits assigned in this study. Our analysis thus opens the way for further kinetic and structural studies to define the mode of allosteric coupling in TRiC.

How is the conformational change propagated around the ring? An interesting speculation arises from recent cryo-EM studies (Cong et al., 2011; Figure S7C) and X-ray studies (Muñoz et al., 2011; Figure S7D) of TRiC in the open state. Both structures are remarkably congruent and reveal a pseudo 4-fold symmetry in the complex driven by local interactions between pairs of specific apical domains. The recently resolved TRiC subunit arrangement (Leitner et al., 2012) allows identification of the subunit pairs with closely interacting apical domains as CCT1/CCT3 and CCT5/CCT7 (Figures 7D, S7C, and S7D, black arrows). Notably, these subunit pairs also serve as interfaces between the high- and low-affinity hemispheres. Thus, the apical domain contacts occurring in the open state may contribute to communicating the power stroke across the apical region of the complex (Figure 7D); however, the directionality of this power stroke remains unclear. In addition, extensive contacts link the equatorial domains of adjacent subunits via a mixed four-stranded beta sheet involving the N and C termini, as well as loops that communicate with the ATP-binding pocket (Pereira et al., 2011). Interestingly, the nucleotide-sensing loop (NSL), which is critical for timing the ATPase cycle (Pereira et al., 2011), contains a conformationally less restrictive serine in the high-affinity subunits (Figure S7E) and a highly conserved, more restrictive threonine in the two lowest-affinity subunits, CCT3 and CCT6. How these differences in the regulatory loop affect the ATPase cycle remains to be determined, but they clearly point to a functional diversification in the subunits depending on their position within the ring.

The TRiC structure (Leitner et al., 2012) also reveals an intricate interaction network within each ring and at the ring-ring interface that is absent in archaeal chaperonins. It is tempting to speculate that these eukaryote-specific contacts help to coordinate ATP-induced conformational changes throughout the ring. Perhaps the most remarkable feature elucidated by the TRiC structure (Leitner et al., 2012) concerns the N terminus of subunit CCT4, which

is pinpointed by our data as the critical regulator of the TRiC ATPase cycle. CCT4 is the only subunit whose N terminus points outward, interdigitating into the interring space (Figure 7D, cyan arrow). In contrast, all N-terminal extensions of the other TRiC subunits point inward and contact the neighboring equatorial domains to mediate inter- and intraring contacts. This evolutionarily conserved CCT4 structural feature, together with the extreme sensitivity of the CCT4 ATP-binding pocket to any mutation, suggests that CCT4 is the key to regulate the ATP-driven conformational cycle, and may help to initiate the power stroke and/or dictate its directionality.

### Implications for TRiC-Mediated Folding, Function, and Regulation

TRiC is unusual as a folding machine because it hydrolyzes ATP very slowly (Pereira et al., 2011; Reissmann et al., 2007) and can fold multidomain proteins with complex topologies that other chaperonins cannot fold (Tian et al., 1995; Yam et al., 2008). These distinct properties may rely on the unique mode of ATP utilization by TRiC. The spatial segregation of ATP usage may organize or provide a sequential mode of substrate release into the central chamber (Rivenzon-Segal et al., 2005), thereby directing the substrate along specific folding trajectories. For instance, reinterpretation of the open TRiC/CCT-tubulin structure (Muñoz et al., 2011) in light of the recently published TRiC subunit arrangement (Leitner et al., 2012) reveals that this substrate associates with subunits CCT5/2/4, which comprise the high-affinity lobe. This raises the possibility of coordinating directional ATP-induced ring closure and substrate release to facilitate polypeptide folding. In addition, this mode of ATP usage may allow TRiC to function under low-energy conditions. Under steady-state conditions, the ATP concentration in yeast and mammalian cells has been estimated to be in the low millimolar range (Hara and Mori, 2006; Richard et al., 1996; Viarengo et al., 1986). However, the ATP concentration has been shown to oscillate in vivo in both mammalian cells (Bertram et al., 2007) and *Saccharomyces cerevisiae* (Richard, 2003) depending on the physiological state. We previously showed that the rate of actin folding by TRiC is the same at 200 μM and 1 mM ATP (Reissmann et al., 2007), indicating that this molecular machine is folding competent even at lower concentrations of ATP. The ability of TRiC to fold substrates in a broad range of ATP concentrations may be an important feature that is hard-wired into the TRiC complex, since it has been implicated in the adaptation to new physiological conditions, such as oxidative stress (Albanèse et al., 2006; Batista-Nascimento et al., 2011) and B cell differentiation (van Anken et al., 2003), where ATP supplies may be constrained. It is tempting to speculate that the ability of TRiC to fully power the cycle through nucleotide binding to only a few high-affinity subunits may allow this chaperonin to reduce ATP consumption while maintaining its essential activity under conditions of low cellular ATP. Intriguingly, even though they are dispensable for function in vivo, the low-affinity subunits still possess the residues required for ATP hydrolysis, even under TRiC-stress conditions. In principle, ATP occupancy of these low-affinity subunits may occur under specific circumstances to regulate TRiC function (Jiang et al., 2011). Interactions with cofactors could serve to adjust ATP occupancy and/or the ATP hydrolysis rate for optimal folding for specific sets of substrates.

The additional layer of complexity in the mechanism of TRiC uncovered here could offer an interesting means of regulation by cofactors and posttranslational modifications (Abe et al., 2009; Liu et al., 2010), which may affect TRiC function during the cell cycle, stress, or aging. Remarkably, TRiC also exhibits a highly asymmetric charge distribution in its central chamber (Leitner et al., 2012). It appears that TRiC exploited its hetero-oligomeric nature to evolve zones with distinct biochemical and functional properties. Understanding the relationships between these characteristics and the substrate binding and folding cycle should reveal how this unique allosteric folding machine achieves folding of its highly complex set of eukaryotic substrates.

## EXPERIMENTAL PROCEDURES

For a more detailed description of the procedures used in this work, see Extended Experimental Procedures.

### Biochemical Methods

Purified bovine TRiC (Feldman et al., 2003) was incubated with α-[$^{32}$P]-ATP or α-[$^{32}$P]-8$N_3$-ATP in the presence or absence of $AlF_x$. 8$N_3$-ATP was crosslinked by UV-photoactivation for 2 min. For stoichiometry measurements, unbound nucleotide was removed with the use of a Sephadex G-50 (Pharmacia) column, followed by scintillation counting and protein concentration measurements. The nucleotide occupancy of TRiC subunits was determined by RP-HPLC separation, followed by scintillation counting or autoradiography of individual fractions. The ability of mutant TRiC complexes to adopt the closed conformation was assessed by incubation with or without 1 mM ATP$AlF_x$ followed by native PAGE and immunoblot against TRiC. To test the activity of the CCT6BND mutant TRiC complex, the corresponding yeast strains were grown to log phase and labeled with 100 μCi/ml $^{35}$S-methionine for 1 min, followed by a chase with 20 mM cold methionine. At the indicated time points, lysates were prepared (see Extended Experimental Procedures) and de novo actin folding was assessed by selective pulldown with immobilized DNaseI as previously described (Thulasiraman et al., 2000).

### Bioinformatic Methods

Homology model building and nucleotide docking were carried out using the Rosetta software package (Chivian and Baker, 2006; Davis and Baker, 2009). Conservation scores were calculated using Rate4site (Pupko et al., 2002) and mapped onto the models using ConSurf (Ashkenazy et al., 2010).

### Yeast Strain Constructions and Growth Experiments

The plasmids and yeast strains used in this study are listed in Table S3 and Table S4, respectively. The CCTx BND, Bnd*, and HYD mutants were generated using the QuickChange approach (Stratagene) from plasmids containing each *cctx* gene under the control of the endogenous promoter (Kabir et al., 2005). A plasmid-shuffling approach was used to generate haploid yeast strains carrying mutant *cctx* alleles. Serial dilutions started with cell suspension from exponentially grown cultures, spotted onto the appropriate media. Stress plates contained 15 μg/ml benomyl. Yeast growth curves were performed by measuring the $OD_{600}$ on an infinite M1000 TECAN plate reader.

## Supplementary Material

Refer to Web version on PubMed Central for supplementary material.

## Acknowledgments

We thank Raul Andino, Dan Gestaut, and Martin Thanbichler for critical readings of the manuscript, and Andreas Bracher for useful discussions. This work was supported by grants from the National Institutes of Health to J.F. L.A.J. is funded by a National Institutes of Health Fellowship. S.R. was funded by the Studienstiftung des Deutschen Volkes. S.R. and A.S.M. purified proteins. S.R. performed the crosslink-HPLC experiments, ATPase assays, and in vivo pulse-chase experiments. A.S.M. performed the stoichiometry experiments. L.A.J. performed the homology model building, conservation score calculations, docking calculations, mutant design, and structural analysis. A.N. and B.C. generated the yeast cctx mutants. B.C. performed the yeast genetic experiments and the native-PAGE experiments to analyze ATP-induced TRiC closure. J.F. designed and interpreted experiments. S.R., L.A.J., and J.F. wrote the manuscript. All authors contributed to preparation of the manuscript.

## References


Abe Y, Yoon SO, Kubota K, Mendoza MC, Gygi SP, Blenis J. p90 ribosomal S6 kinase and p70 ribosomal S6 kinase link phosphorylation of the eukaryotic chaperonin containing TCP-1 to growth factor, insulin, and nutrient signaling. J Biol Chem. 2009; 284:14939–14948. [PubMed: 19332537]

Albanèse V, Yam AY, Baughman J, Parnot C, Frydman J. Systems analyses reveal two chaperone networks with distinct functions in eukaryotic cells. Cell. 2006; 124:75–88. [PubMed: 16413483]

Amit M, Weisberg SJ, Nadler-Holly M, McCormack EA, Feldmesser E, Kaganovich D, Willison KR, Horovitz A. Equivalent mutations in the eight subunits of the chaperonin CCT produce dramatically different cellular and gene expression phenotypes. J Mol Biol. 2010; 401:532–543. [PubMed: 20600117]

Archibald JM, Blouin C, Doolittle WF. Gene duplication and the evolution of group II chaperonins: implications for structure and function. J Struct Biol. 2001; 135:157–169. [PubMed: 11580265]

Ashkenazy H, Erez E, Martz E, Pupko T, Ben-Tal N. ConSurf 2010: calculating evolutionary conservation in sequence and structure of proteins and nucleic acids. Nucleic Acids Res. 2010; 38(Web Server issue):W529–33. [PubMed: 20478830]

Batista-Nascimento L, Neef DW, Liu PC, Rodrigues-Pousada C, Thiele DJ. Deciphering human heat shock transcription factor 1 regulation via post-translational modification in yeast. PLoS ONE. 2011; 6:e15976. [PubMed: 21253609]

Bertram R, Satin LS, Pedersen MG, Luciani DS, Sherman A. Interaction of glycolysis and mitochondrial respiration in metabolic oscillations of pancreatic islets. Biophys J. 2007; 92:1544–1555. [PubMed: 17172305]

Bigotti MG, Clarke AR. Chaperonins: the hunt for the Group II mechanism. Arch Biochem Biophys. 2008; 474:331–339. [PubMed: 18395510]

Bochkareva ES, Lissin NM, Flynn GC, Rothman JE, Girshovich AS. Positive cooperativity in the functioning of molecular chaperone GroEL. J Biol Chem. 1992; 267:6796–6800. [PubMed: 1348056]

Booth CR, Meyer AS, Cong Y, Topf M, Sali A, Ludtke SJ, Chiu W, Frydman J. Mechanism of lid closure in the eukaryotic chaperonin TRiC/CCT. Nat Struct Mol Biol. 2008; 15:746–753. [PubMed: 18536725]

Camasses A, Bogdanova A, Shevchenko A, Zachariae W. The CCT chaperonin promotes activation of the anaphase-promoting complex through the generation of functional Cdc20. Mol Cell. 2003; 12:87–100. [PubMed: 12887895]

Chivian D, Baker D. Homology modeling using parametric alignment ensemble generation with consensus and energy-based model selection. Nucleic Acids Res. 2006; 34:e112. [PubMed: 16971460]

Cong Y, Schroder GF, Meyer AS, Jakana J, Ma B, Dougherty MT, Schmid MF, Reissmann S, Levitt M, Ludtke SL, et al. Symmetry-free cryo-EM structures of the chaperonin TRiC along its ATPase-driven conformational cycle. EMBO J. 2011; 31:720–730. [PubMed: 22045336]

Davis IW, Baker D. RosettaLigand docking with full ligand and receptor flexibility. J Mol Biol. 2009; 385:381–392. [PubMed: 19041878]

Dekker C, Roe SM, McCormack EA, Beuron F, Pearl LH, Willison KR. The crystal structure of yeast CCT reveals intrinsic asymmetry of eukaryotic cytosolic chaperonins. EMBO J. 2011; 30:3078–3090. [PubMed: 21701561]

Ditzel L, Löwe J, Stock D, Stetter KO, Huber H, Huber R, Steinbacher S. Crystal structure of the thermosome, the archaeal chaperonin and homolog of CCT. Cell. 1998; 93:125–138. [PubMed: 9546398]

Douglas NR, Reissmann S, Zhang J, Chen B, Jakana J, Kumar R, Chiu W, Frydman J. Dual action of ATP hydrolysis couples lid closure to substrate release into the group II chaperonin chamber. Cell. 2011; 144:240–252. [PubMed: 21241893]

Feldman DE, Spiess C, Howard DE, Frydman J. Tumorigenic mutations in VHL disrupt folding in vivo by interfering with chaperonin binding. Mol Cell. 2003; 12:1213–1224. [PubMed: 14636579]

Fenton WA, Kashi Y, Furtak K, Horwich AL. Residues in chaperonin GroEL required for polypeptide binding and release. Nature. 1994; 371:614–619. [PubMed: 7935796]

Gutsche I, Mihalache O, Baumeister W. ATPase cycle of an archaeal chaperonin. J Mol Biol. 2000; 300:187–196. [PubMed: 10864508]

Hara KY, Mori H. An efficient method for quantitative determination of cellular ATP synthetic activity. J Biomol Screen. 2006; 11:310–317. [PubMed: 16490767]

Hartl FU, Bracher A, Hayer-Hartl M. Molecular chaperones in protein folding and proteostasis. Nature. 2011; 475:324–332. [PubMed: 21776078]

Horwich AL, Farr GW, Fenton WA. GroEL-GroES-mediated protein folding. Chem Rev. 2006; 106:1917–1930. [PubMed: 16683761]

Horwich AL, Fenton WA, Chapman E, Farr GW. Two families of chaperonin: physiology and mechanism. Annu Rev Cell Dev Biol. 2007; 23:115–145. [PubMed: 17489689]

Jiang Y, Douglas NR, Conley NR, Miller EJ, Frydman J, Moerner WE. Sensing cooperativity in ATP hydrolysis for single multisubunit enzymes in solution. Proc Natl Acad Sci USA. 2011; 108:16962–16967. [PubMed: 21896715]

Kabir MA, Kaminska J, Segel GB, Bethlendy G, Lin P, Della Seta F, Blegen C, Swiderek KM, Zoładek T, Arndt KT, Sherman F. Physiological effects of unassembled chaperonin Cct subunits in the yeast Saccharomyces cerevisiae. Yeast. 2005; 22:219–239. [PubMed: 15704212]

Kafri G, Willison KR, Horovitz A. Nested allosteric interactions in the cytoplasmic chaperonin containing TCP-1. Protein Sci. 2001; 10:445–449. [PubMed: 11266630]

Kim S, Willison KR, Horwich AL. Cystosolic chaperonin subunits have a conserved ATPase domain but diverged polypeptide-binding domains. Trends Biochem Sci. 1994; 19:543–548. [PubMed: 7846767]

Kitamura A, Kubota H, Pack CG, Matsumoto G, Hirayama S, Takahashi Y, Kimura H, Kinjo M, Morimoto RI, Nagata K. Cytosolic chaperonin prevents polyglutamine toxicity with altering the aggregation state. Nat Cell Biol. 2006; 8:1163–1170. [PubMed: 16980958]

Leitner A, Joachimiak LA, Bracher A, Mönkemeyer L, Walzthoeni T, Chen B, Pechmann S, Holmes S, Cong Y, Ma B, et al. The molecular architecture of the eukaryotic chaperonin TRiC/CCT. Structure. 2012; 20:814–825. [PubMed: 22503819]

Lin P, Cardillo TS, Richard LM, Segel GB, Sherman F. Analysis of mutationally altered forms of the Cct6 subunit of the chaperonin from Saccharomyces cerevisiae. Genetics. 1997; 147:1609–1633. [PubMed: 9409825]

Liu B, Larsson L, Caballero A, Hao X, Oling D, Grantham J, Nyström T. The polarisome is required for segregation and retrograde transport of protein aggregates. Cell. 2010; 140:257–267. [PubMed: 20141839]

Meyer AS, Gillespie JR, Walther D, Millet IS, Doniach S, Frydman J. Closing the folding chamber of the eukaryotic chaperonin requires the transition state of ATP hydrolysis. Cell. 2003; 113:369–381. [PubMed: 12732144]

Muñoz IG, Yébenes H, Zhou M, Mesa P, Serna M, Park AY, Bragado-Nilsson E, Beloso A, de Cárcer G, Malumbres M, et al. Crystal structure of the open conformation of the mammalian chaperonin CCT in complex with tubulin. Nat Struct Mol Biol. 2011; 18:14–19. [PubMed: 21151115]

Neef DW, Turski ML, Thiele DJ. Modulation of heat shock transcription factor 1 as a therapeutic target for small molecule intervention in neurodegenerative disease. PLoS Biol. 2010; 8:e1000291. [PubMed: 20098725]

Pereira JH, Ralston CY, Douglas NR, Kumar R, Lopez T, McAndrew RP, Knee KM, King JA, Frydman J, Adams PD. Mechanism of nucleotide sensing in group II chaperonins. EMBO J. 2011; 31:731–740. [PubMed: 22193720]

Pupko T, Bell RE, Mayrose I, Glaser F, Ben-Tal N. Rate4Site: an algorithmic tool for the identification of functional regions in proteins by surface mapping of evolutionary determinants within their homologues. Bioinformatics. 2002; 18(Suppl 1):S71–S77. [PubMed: 12169533]

Reissmann S, Parnot C, Booth CR, Chiu W, Frydman J. Essential function of the built-in lid in the allosteric regulation of eukaryotic and archaeal chaperonins. Nat Struct Mol Biol. 2007; 14:432–440. [PubMed: 17460696]

Richard P. The rhythm of yeast. FEMS Microbiol Rev. 2003; 27:547–557. [PubMed: 14550945]

Richard P, Teusink B, Hemker MB, Van Dam K, Westerhoff HV. Sustained oscillations in free-energy state and hexose phosphates in yeast. Yeast. 1996; 12:731–740. [PubMed: 8813760]

Rivenzon-Segal D, Wolf SG, Shimon L, Willison KR, Horovitz A. Sequential ATP-induced allosteric transitions of the cytoplasmic chaperonin containing TCP-1 revealed by EM analysis. Nat Struct Mol Biol. 2005; 12:233–237. [PubMed: 15696173]

Rye HS, Roseman AM, Chen S, Furtak K, Fenton WA, Saibil HR, Horwich AL. GroEL-GroES cycling: ATP and nonnative polypeptide direct alternation of folding-active rings. Cell. 1999; 97:325–338. [PubMed: 10319813]

Spiess C, Meyer AS, Reissmann S, Frydman J. Mechanism of the eukaryotic chaperonin: protein folding in the chamber of secrets. Trends Cell Biol. 2004; 14:598–604. [PubMed: 15519848]

Spiess C, Miller EJ, McClellan AJ, Frydman J. Identification of the TRiC/CCT substrate binding sites uncovers the function of subunit diversity in eukaryotic chaperonins. Mol Cell. 2006; 24:25–37. [PubMed: 17018290]

Taguchi H, Tsukuda K, Motojima F, Koike-Takeshita A, Yoshida M. BeF(x) stops the chaperonin cycle of GroEL-GroES and generates a complex with double folding chambers. J Biol Chem. 2004; 279:45737–45743. [PubMed: 15347650]

Tam S, Geller R, Spiess C, Frydman J. The chaperonin TRiC controls polyglutamine aggregation and toxicity through subunit-specific interactions. Nat Cell Biol. 2006; 8:1155–1162. [PubMed: 16980959]

Thulasiraman V, Yang CF, Frydman J. In vivo newly translated polypeptides are sequestered in a protected folding environment. EMBO J. 1999; 18:85–95. [PubMed: 9878053]

Thulasiraman V, Ferreyra RG, Frydman J. Monitoring actin folding. Purification protocols for labeled proteins and binding to DNase I-sepharose beads. Methods Mol Biol. 2000; 140:161–167. [PubMed: 11484485]

Tian G, Vainberg IE, Tap WD, Lewis SA, Cowan NJ. Specificity in chaperonin-mediated protein folding. Nature. 1995; 375:250–253. [PubMed: 7746329]

Tyedmers J, Mogk A, Bukau B. Cellular strategies for controlling protein aggregation. Nat Rev Mol Cell Biol. 2010; 11:777–788. [PubMed: 20944667]

van Anken E, Romijn EP, Maggioni C, Mezghrani A, Sitia R, Braakman I, Heck AJ. Sequential waves of functionally related proteins are expressed when B cells prepare for antibody secretion. Immunity. 2003; 18:243–253. [PubMed: 12594951]

Viarengo A, Secondini A, Scoppa P, Orunesu M. A rapid HPLC method for determination of adenylate energy charge. Experientia. 1986; 42:1234–1235. [PubMed: 3780947]

Weiss C, Goloubinoff P. A mutant at position 87 of the GroEL chaperonin is affected in protein binding and ATP hydrolysis. J Biol Chem. 1995; 270:13956–13960. [PubMed: 7775456]

Yam AY, Xia Y, Lin HT, Burlingame A, Gerstein M, Frydman J. Defining the TRiC/CCT interactome links chaperonin function to stabilization of newly made proteins with complex topologies. Nat Struct Mol Biol. 2008; 15:1255–1262. [PubMed: 19011634]

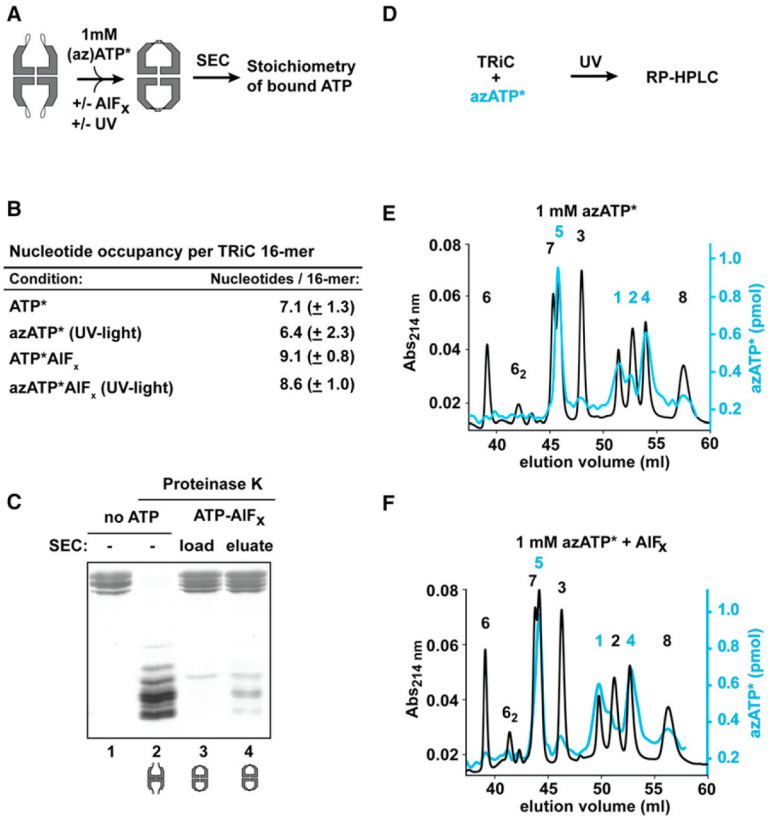


**Figure 1. Substoichiometric ATP Binding in the Eukaryotic Chaperonin TRiC**

(A) Experimental scheme.

(B) Summary of stoichiometry results. Standard deviation is displayed in brackets.

(C) Bovine TRiC complexes incubated with ATP and $AlF_x$ remain closed during the SEC procedure applied to determine TRiC-nucleotide stoichiometry. The indicated TRiC-nucleotide complexes were subjected to Proteinase K treatment before (load, lane 3) or after (eluate, lane 4) SEC. To assay protease sensitivity, the reactions were resolved by SDS-PAGE and the proteins were detected by silver stain. The helical protrusions in the open conformation of TRiC are unstructured and protease sensitive; therefore, when treated with protease, the subunits are cleaved in half (lane 2), and when the TRiC complex is closed, the subunits are protease resistant (Meyer et al., 2003) (lanes 3 and 4).

(D) Experimental scheme for (E) and (F).

(E and F) Separation of bovine TRiC subunits by RP-HPLC after crosslinking with (E) 1 mM azATP* and (F) 1 mM azATPAlFx. Black: UV profile; blue: coeluting [$^{32}$P] nucleotide profile. Numbers refer to TRiC/CCT subunit identity (Spiess et al., 2006). Blue numbers: subunits coeluting with nucleotide.

See also Figures S1 and S2 and Table S1.

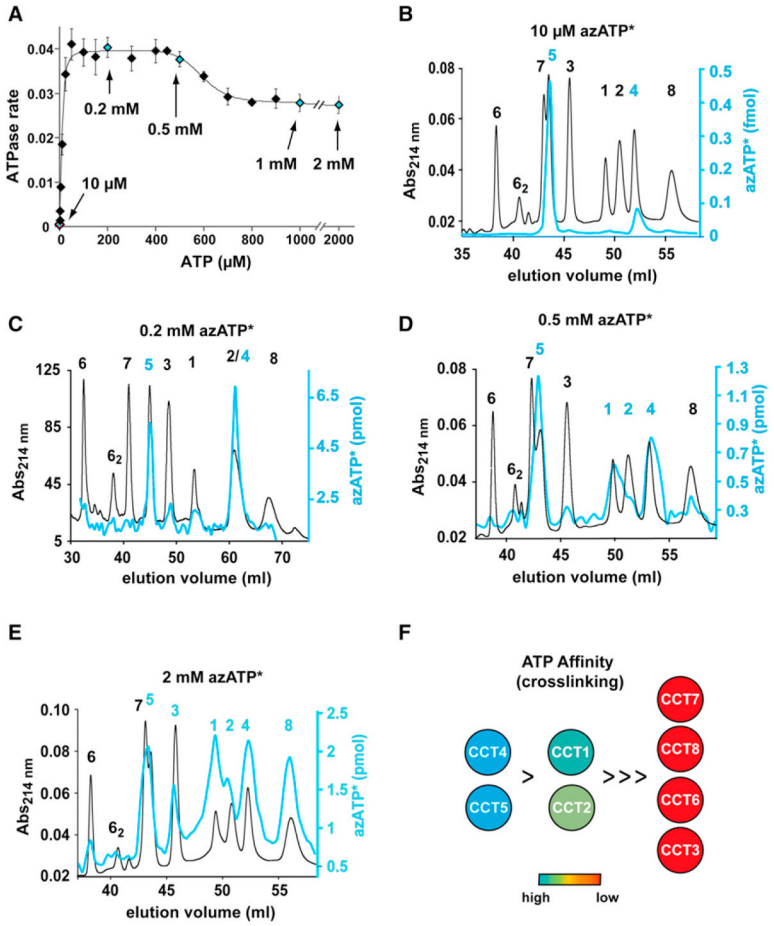


**Figure 2. Differential ATP Binding within the Paralogous TRiC/CCT Subunits**

(A) Initial velocities of the ATP hydrolysis rate of bovine TRiC blotted against the corresponding ATP concentrations (taken from Reissmann et al., 2007). The arrows point to the ATP concentrations at which the crosslink experiments were performed. Each data point shows the average of at least three independent experiments. Error bars represent the SEM. (B–E) The subunits in bovine TRiC display different affinities for ATP. Separation of the subunits by RP-HPLC after crosslinking with α-[$^{32}$P]-8N$_3$-ATP at 10 μM ATP (B), 0.2 mM ATP (C), 0.5 mM ATP (D), and 2 mM ATP (E). Black: UV profile; blue: coeluting [$^{32}$P] nucleotide profile. Numbers refer to TRiC/CCT subunit identity (Spiess et al., 2006). Blue numbers: subunits coeluting with nucleotide. (F) ATP occupancy of CCT1–CCT8 as a function of concentration. The color-coding bar indicates the coloring scheme. See also Figures S1 and S2.

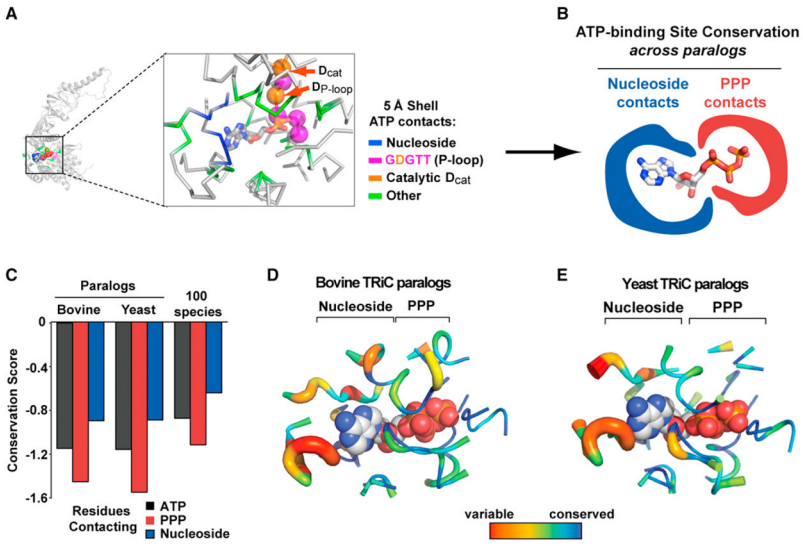


**Figure 3. Conservation of Paralogous TRiC/CCT ATP Binding Pockets**

(A) Group II chaperonin active site; 5 Å shell around the nucleotide. Green: nucleoside contacts; blue: P loop (GDGTT-motif); pink: $D_{P\ loop}$; orange: catalytic $D_{cat}$.

(B) Schematic representation of the two distinct regions in the ATP-binding pocket, illustrating the nucleoside and triphosphate contacts, colored in blue and red, respectively.

(C) Average conservation scores of amino acids within the 5 Å shell around the entire nucleotide (ATP, black bars), the triphosphate (PPP, red bars), and the nucleoside (blue bars) calculated for the paralogous subunits of bovine and yeast TRiC, as well as for TRiC/CCT sequences for each of the eight subunits from 100 different species.

(D) Bovine CCT1 active site colored according to conservation scores (Ashkenazy et al., 2010) calculated for bovine CCT1–CCT8.

(E) Yeast CCT1 active site colored according to conservation scores (Ashkenazy et al., 2010) calculated for yeast CCT1–CCT8. The backbone thickness is proportional to the conservation score.

See also Figure S3.

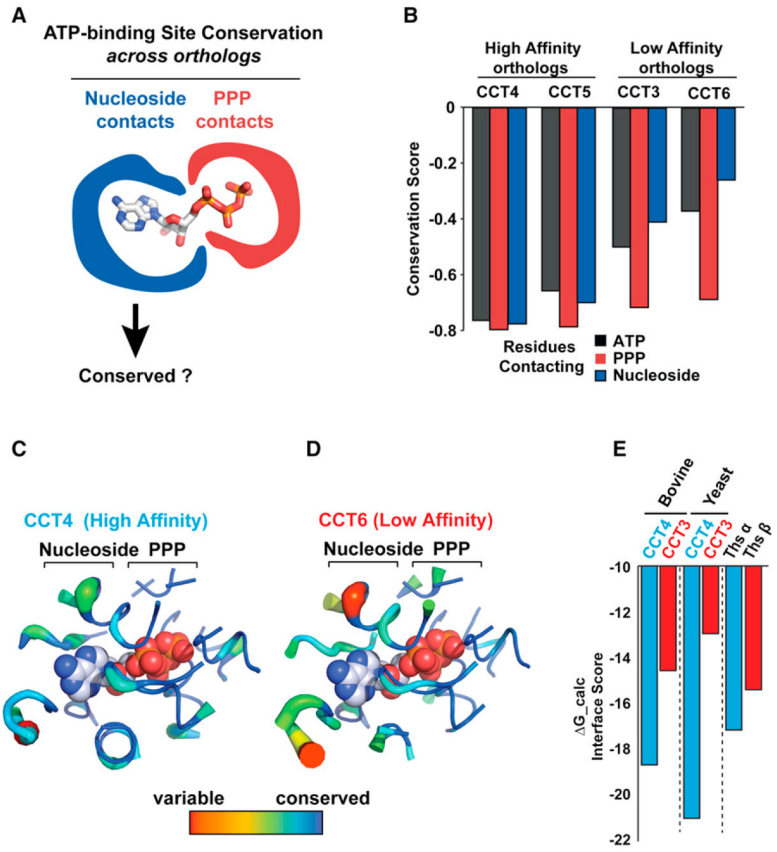


**Figure 4. Evolutionary Conservation and Energetics of Orthologous TRiC/CCT Subunit Active Sites**

(A) Schematic representation of the two distinct regions in the ATP-binding pocket, illustrating the nucleoside and triphosphate contacts, colored in blue and red, respectively.

(B) Average conservation scores of amino acids within the 5 Å shell around the entire nucleotide (ATP, black bars), the triphosphate (PPP, red bars) and the nucleoside (blue bars) calculated for the 100 orthologous sequences of high-affinity (CCT4 and CCT5) and low-affinity (CCT6 and CCT3) subunits.

(C and D) Average conservation scores (Ashkenazy et al., 2010) calculated for 100 orthologous sequences for CCT4 (high affinity) and CCT6 (low affinity) mapped onto the active site of the respective subunits. The backbone thickness is proportional to the conservation score.

(E) Nucleotide-docking experiments. The $\Delta G_{calc}$ (interface_score; Davis and Baker, 2009) was used to estimate the free energy for ATP binding to the active site of representative high-affinity (blue bars) and low-affinity (red bars) subunits using homology models of bovine TRiC subunits (see Extended Experimental Procedures for details) and yeast TRiC subunits (PDB code: 4D8Q), as well as to α and β subunits (PDB code: 1A6E).

See also Figure S4.

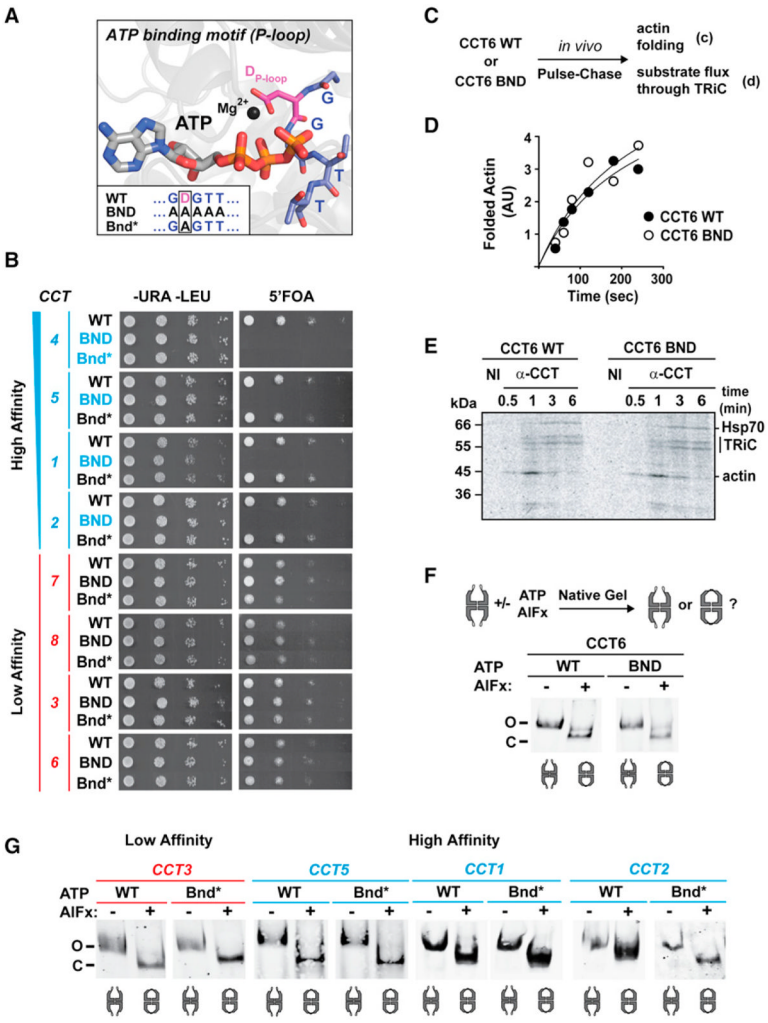


**Figure 5. Functional Relevance of ATP Binding in Each Paralogous Yeast TRiC Subunit**

(A) CCTx active site highlighting key residues and mutations involved in ATP binding (blue: P loop (GDGTT); pink: except $D_{Ploop}$). BND, GDGTT/AAAAA; Bnd*, $D_{Ploop}$A.

(B) Viability of *cctx*-deletion strains carrying the wild-type (WT), BND, or Bnd* CCTx variants. Right panel: 5′FOA selection plates (to reveal the mutant phenotype). Left panel: control plates (to assess total cells analyzed).

(C–E) ATP binding to CCT6 is not required for efficient actin folding in the cytosol. (C) Experimental strategy. (D) Rate of cotranslational folding of pulse-labeled actin in yeast *cct6*-deletion strains expressing either WT CCT6 or the mutant version CCT6 BND. Folded actin was isolated at the indicated time points by DNaseI pulldown, separated on SDS-PAGE, and quantified after autoradiographic exposure of the gel. (E) The association and dissociation kinetics of pulse-labeled actin and TRiC were determined by TRiC immunoprecipitation in yeast *cct6*-deletion strains expressing either WT CCT6 or the mutant version, CCT6 BND. An autoradiogram is shown, and radiolabeled bands corresponding to TRiC, actin, and Hsp70 are marked. NI, no antibody added.

(F) Yeast lysates prepared from the indicated strains were incubated with 1 mM ATP and AlFx to induce the kinetically stable, fully closed conformation in TRiC. After separation of the complexes by native PAGE, the TRiC complex was detected by western blot using CCT-specific antibodies. Because the ATPAlFx-induced, double-closed complex migrates farther

into the native gel than the complex in the open conformation, this assay can determine whether the respective mutations interfere with the conformational cycle of TRiC. O: open conformation; C: closed conformation.
(G) Native-PAGE analysis of ATP-induced TRiC closure in Bnd* mutants.
See also Figure S5 and Table S2.

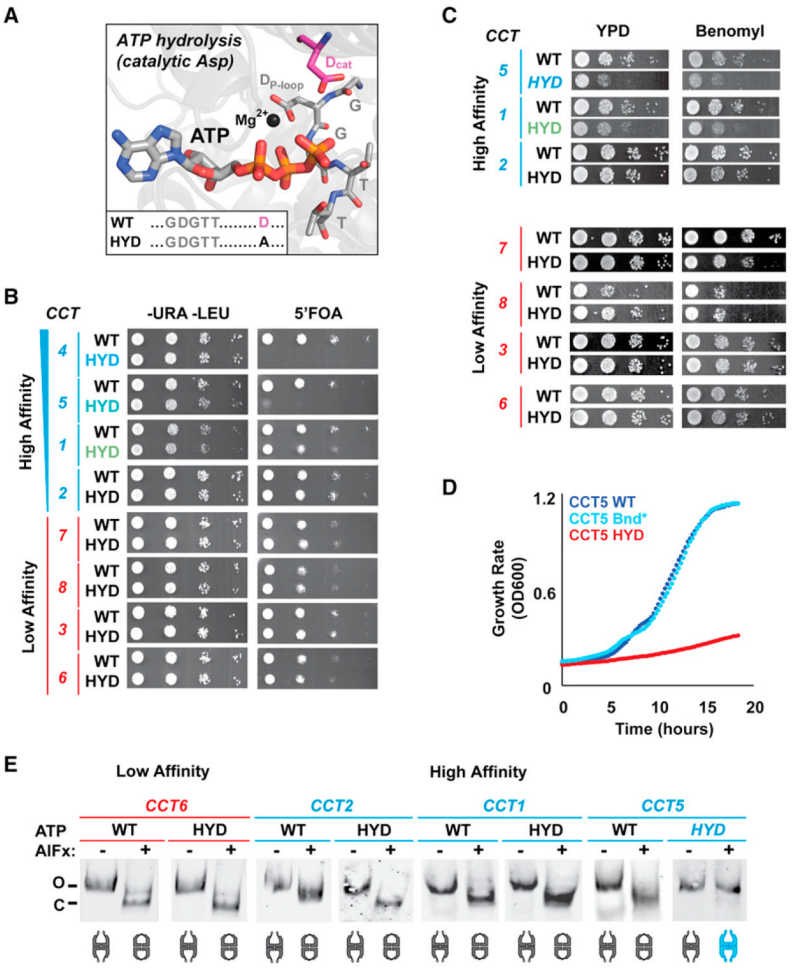


**Figure 6. Functional Relevance of ATP Hydrolysis in Each Paralogous Yeast TRiC Subunit**

(A) CCTx active site highlighting key residues and mutations involved in ATP hydrolysis. Gray: P loop (GDGTT); pink: $D_{cat}$. HYD: $D_{cat}A$.

(B) Viability of *cctx*-deletion strains carrying the *cctx* WT or HYD mutant. Right panel: 5′FOA selection plates (to reveal the mutant phenotype). Left panel: control plates (to assess total cells analyzed).

(C) Benomyl sensitivity of *cctx*-deletion strains carrying the *cctx* WT or HYD mutants. Right panel: benomyl. Left panel: control for total cells.

(D) Liquid culture growth assay for CCT5 WT, CCT5 HYD, and CCT5 Bnd* (shown as dark blue, red, and light blue curves, respectively), demonstrating the growth defect due to the hydrolysis mutation in CCT5 (see analysis of growth curves for each strain in Table S2).

(E) Native-PAGE analysis of ATP-induced TRiC closure in HYD mutants. See also Figure S6.

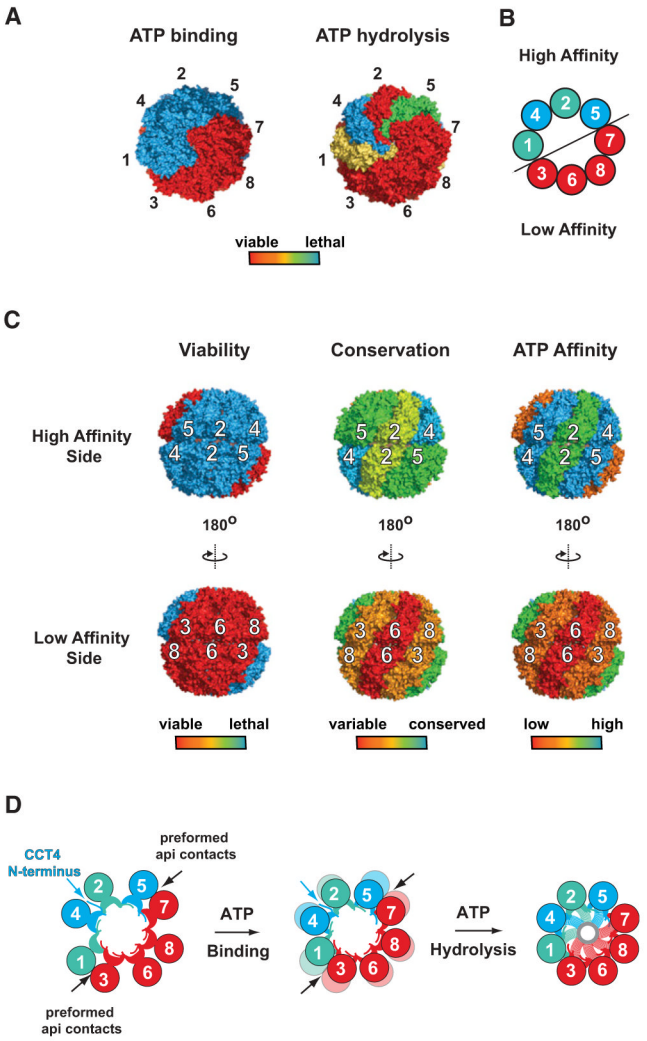


**Figure 7. High- and Low-Affinity Subunits Segregate into Two Distinct Hemispheres on the TRiC Structure to Drive an Asymmetric Conformational Cycle**

The TRiC structure with the subunits arranged in the order described in the text is shown in surface representation (Pymol). Each subunit in the complex is colored according to the indicated properties.

(A) Top view shows the viability of ATP binding and ATP hydrolysis mutants.

(B) Schematic representation of the spatial segregation of the high- and low-affinity subunits in the TRiC structure.

(C) Side view for viability (left panel), nucleoside conservation (middle panel), and azATP crosslink occupancy (right panel).

(D) Proposed model for the functional role of the high- and low-affinity hemispheres in the asymmetric conformational cycle.

See also Figure S7.